

# Nonradioactive Iodide Effectively Induces Apoptosis in Genetically Modified Lung Cancer Cells<sup>1</sup>

Ling Zhang, Sherven Sharma, Li X. Zhu, Takahiko Kogai, Jerome M. Hershman, Gregory A. Brent, Steven M. Dubinett,<sup>2</sup> and Min Huang<sup>2</sup>

Division of Pulmonary and Critical Care Medicine [L. Z., S. S., L. X. Z., S. M. D., M. H.], Division of Endocrinology and Metabolism, Department of Medicine [T. K., J. M. H., G. A. B.], Lung Cancer Research Program of the Jonsson Comprehensive Cancer Center [S. M. D.], and Department of Pathology, David Geffen School of Medicine [M. H.], University of California Los Angeles and Veterans Affairs Greater Los Angeles Healthcare System, California 90073

## ABSTRACT

We assessed a nonradioactive approach to induce apoptosis in non-small cell lung cancer by a novel iodide uptake and retention mechanism. To enhance tumor apoptosis, we transduced non-small cell lung cancer cells with retroviral vectors containing the sodium iodide symporter (*NIS*) and thyroperoxidase (*TPO*) genes. Expression of *NIS* and *TPO* facilitated concentration of iodide in tumors. As a consequence of the marked increase in intracellular levels of iodide, apoptosis was seen in >95% of *NIS/TPO*-modified lung cancer cells. Intraperitoneal injection of potassium iodide resulted in significant tumor volume reduction in *NIS/TPO*-modified tumor xenografts without apparent adverse effects in SCID mice. Iodide induced an increase in the level of reactive oxygen species. Iodide-induced apoptosis is sensitive to *N*-acetylcysteine inhibition, suggesting an important role by reactive oxygen species in this apoptotic process. In addition, iodide-induced apoptosis is associated with overexpression of *CDKN1A* (*p21/Waf1*) and down-regulation of survivin at both mRNA and protein levels. This is the first report demonstrating that a therapeutic dose of nonradioactive iodide has potent efficacy and high selectivity against lung cancer when used in combination with genetic modification of cancer cells to express the *NIS/TPO* genes.

## INTRODUCTION

Lung cancer is the leading cause of cancer death in both men and women in the United States (1–3). Currently, there is no reliable and effective therapy for patients with inoperable NSCLC,<sup>3</sup> and the prognosis remains very poor. Therefore, development of new therapeutic strategies for the treatment of lung cancer is clearly needed.

The ability to concentrate iodide is a fundamental property of the normally functioning thyroid gland and represents the first step in the synthesis of thyroid hormones. *NIS* plays a key role in thyroid hormone production by efficiently accumulating iodide from the circulation into the thyrocytes against an electrochemical gradient (4–8). The *NIS* gene, expressed by the thyroid cells, is also found in salivary gland, choroid plexus, gastric parietal cells, and lactating breast (5–7, 9). *TPO* catalyzes iodination of proteins and promotes iodide accumulation within thyrocytes (10, 11).

We reported previously that genetic modification of NSCLC cells with *NIS* and *TPO* genes led to concentration of radioiodide and

enhanced tumor cell apoptosis (12). Our rationale for choosing the *NIS* and *TPO* genes is based on the fact that intracellular iodide retention in the normal thyroid is enhanced by *TPO*-mediated incorporation of iodide into protein. Although this *TPO*-enhanced *NIS*-based gene therapy (12) produces concentration of radioiodide in cancer cells, radiation-induced toxicity to normal tissues could limit its clinical application.

Previous studies have shown that excess iodide induces apoptosis in thyroid cells (13). To improve the iodide concentrating capacity of lung cancer cells, we transduced tumor cells with retroviral vectors containing functional *NIS* and *TPO* genes to take advantage of the effects of nonradioactive iodide. The iodide concentrating capacity in the transduced lung cancer cell clones was markedly increased, up to 320-fold as determined by <sup>125</sup>I uptake assays. We demonstrate here for the first time that nonradioactive iodide effectively induces apoptosis in the *NIS/TPO*-modified lung cancer cells.

## MATERIALS AND METHODS

**Cell Culture.** Human lung undifferentiated large cell carcinoma cell line H1299 was obtained from American Type Culture Collection (Rockville, MD). The cells were grown at 37°C under an atmosphere of 5% CO<sub>2</sub> in air as monolayers in 25-cm<sup>2</sup> tissue culture flasks containing 5.0 ml of RPMI 1640 supplemented with 10% fetal bovine serum, 100 units/ml penicillin/streptomycin solution and 2 mM glutamine (JRH Biosciences, Lenexa, KS).

**Mice.** Pathogen-free 6–8-week-old female SCID/beige CB17 mice (T-, B-, natural killer-cell deficient) were obtained from University of California Los Angeles and maintained in cages housed in laminar flow hoods under pathogen-free conditions in the West Los Angeles VA Animal Research Facility. All of the studies were approved by the Institutional Animal Research Committee.

**Retroviral Vector Construction and the Transduction of H1299 Cells.** Human *NIS* and *TPO* plasmid vectors were described previously (12). Retroviral vectors pLHCX containing a hygromycin-selection marker and pLNCX containing a neomycin-selection marker were obtained from Clontech Laboratories, Inc. (Palo Alto, CA). The retroviral *NIS* and *TPO* vectors were constructed by the insertion of the *NIS* gene into the pLHCX and the *TPO* gene into the pLNCX vectors. After transfection to the PT-67 retroviral packaging cell line by a liposomal-mediated method (Effectene method; Qiagen Inc., Valencia, CA), the supernatants containing high-titer of retroviruses expressing *NIS* or *TPO* were collected to transduce H1299 cells. Single clones of genetically modified H1299 cells were selected with appropriate antibiotic resistant markers. The clones were additionally characterized to confirm the presence of functional *NIS* and *TPO* genes by RT-PCR and <sup>125</sup>I uptake assays.

**Detection of *NIS* and *TPO* by RT-PCR.** We used the following primer pairs for the detection of human *NIS* and *TPO* by RT-PCR: 5'-GCT GAG GAC TTC TTC ACC GGG GGC CG-3' (*NIS* sense primer); 5'-GTC AGG GTT AAA GTC CAT GAG GTT G-3' (*NIS* antisense primer); 5'-CAT GTA CGC CAC GAT GCA GAG A-3' (*TPO* sense primer); and 5'-CTG TGG TGT GAA CGC GAT GTC G-3' (*TPO* antisense primer). The *NIS* primer pairs correspond to the coding region 349–374 and 930–906, respectively, and the *TPO* 199–218 and 778–757, respectively. The amplified products are 558 bp in length for *NIS* and 579 bp for *TPO*. Total RNA was isolated with TRIzol reagents (Invitrogen Corp., Carlsbad, CA). The RT-PCR was performed for 35 cycles of amplification using a PTC-100–60 thermal cycler (MJ Research, Inc., Watertown, MA). The PCR products from each reaction were analyzed by 1.5% agarose/ethidium bromide gel electrophoresis.

Received 1/29/03; revised 5/28/03; accepted 6/4/03.

The costs of publication of this article were defrayed in part by the payment of page charges. This article must therefore be hereby marked *advertisement* in accordance with 18 U.S.C. Section 1734 solely to indicate this fact.

<sup>1</sup> Supported by the University of California Los Angeles Specialized Programs of Research Excellence in Lung Cancer, NIH P50 CA90388, R01 CA085686 (to S. M. D.), Medical Research Funds from the Department of Veteran Affairs, and the Tobacco-Related Disease Research Program of the University of California.

<sup>2</sup> To whom requests for reprints should be addressed, at University of California Los Angeles, West Los Angeles VA, Building 114, Room 103, Los Angeles, CA 90073. E-mail: minhuang@ucla.edu (to M. H.) or UCLA Lung Cancer Research Program, 10833 Le Conte Avenue, 37-131 CHS Los Angeles, CA 90095. E-mail: sdubinett@mednet.ucla.edu (to S. M. D.).

<sup>3</sup> The abbreviations used are: NSCLC, non-small cell lung cancer; *NIS*, sodium iodide symporter; *TPO*, thyroperoxidase; RT-PCR, reverse transcription-PCR; TUNEL, terminal deoxynucleotidyl transferase-mediated nick end labeling; NMP, nuclear matrix protein; DCFH-DA, 5,6-carboxy-2',7'-dichlorofluorescein diacetate; ROS, reactive oxygen species; KI, potassium iodide; FACS, fluorescence-activated cell sorter; TNF, tumor necrosis factor.

**<sup>125</sup>I Uptake and Retention Assays.** The <sup>125</sup>I was obtained from Amersham Pharmacia Biotech (Piscataway, NJ). The methods for <sup>125</sup>I uptake and retention assays were described previously (12). To determine <sup>125</sup>I uptake *in vivo*, SCID mice bearing genetically modified tumors were given 1  $\mu$ Ci of <sup>125</sup>I per mouse by intraperitoneal injection. Three h after administration of <sup>125</sup>I (1  $\mu$ Ci/mouse) by i.p. injection, tumors from each group of mice were removed and weighed, and the tumor-associated radioactivity was determined as <sup>125</sup>I uptake/g of tumor weight by a gamma counter. There were no statistically significant differences in tumor size seen in different groups of animals before <sup>125</sup>I was administered.

**Apoptosis Assays.** Apoptosis was quantified by measuring the levels of cellular dye retention within apoptotic cells using an APOPercentage apoptosis assay kit (Accurate Chemical & Scientific Corporation, New York, NY). The APOPercentage method uses a specially designed dye that is selectively imported and accumulated by cells that are undergoing apoptosis (14). The Klenow-FragEL DNA fragmentation method (Oncogene Research Products, Cambridge, MA) allows for the detection of free 3'-OH groups at the ends of DNA fragments generated by apoptotic endonucleases (15). The TUNEL Apoptosis Detection kit was obtained from Upstate Biotechnology Inc. (Waltham, MA). The TUNEL assay is a well-documented method for the detection of DNA fragmentation (16). NMPs ELISA kit was obtained from Oncogene Research Products (Cambridge, MA). NMPs are released from apoptotic cells (12). In this assay, the amount of released NMPs is a function of the number of apoptotic cells. Apoptosis of tumor xenografts was assessed by microscopic examination of Klenow-FragEL-stained sections with a calibrated graticule (a 1-cm<sup>2</sup> grid subdivided into 100 1 mm<sup>2</sup> squares). A grid square stained in brown occupying >50% of its area was scored as positive, and the total number of positive squares was determined as described previously (17). Twenty separate fields from the histological sections of the tumors were examined under high-power ( $\times 20$  objective). GEArray Q series human stress and toxicity pathway finder and GEArray Q series human apoptosis kits were obtained from SuperArray Inc. (Bethesda, MD). Specific monoclonal antibodies to *CDKN1A* and survivin were obtained from Novus Biologicals Inc. (Littleton, CO). *CDKN1A* and survivin protein levels were determined by ELISA as described previously (17).

**Determination of ROS Level by FACScan.** DCFH-DA was obtained from Molecular Probes, Inc. (Eugene, OR). DCFH-DA is an oxidation-sensitive fluorescent chemical compound readily taken up by the cells and deacylated to a nonfluorescent form (DCFH; Ref. 13). DCFH is oxidized by ROS to a fluorescent form, which can be measured by FACScan. The fluorescent intensity in a cell population is proportional to the ROS level within the cells.

***In Vivo* Nonradioactive Iodide Therapeutic Model for Lung Cancer.** *In vivo* experiments were repeated twice using 8–12 mice per group. Five  $\times 10^6$  exponentially growing genetically modified H1299*NIS/TPO* cells or H1299CV cells as controls were inoculated s.c. on the right suprascapular area in SCID mice. When tumors reached ~5 mm in diameter, mice were administered 100  $\mu$ l of KI (50 mg/ml) per mouse/day, five times a week by i.p. injection. Tumor growth was monitored by measuring two bisecting diameters of each tumor with a caliper twice a week. The tumor volume was calculated using the formula (0.4) (*ab*<sup>2</sup>), with *a* as the larger diameter and *b* as the smaller diameter. Mice were euthanized by day 26 after KI administration. Tumors of each group were completely removed, weighed, photographed, and fixed in 10% formalin/PBS for histological examination.

**Statistical Analysis.** *In vitro* results are presented as means  $\pm$  SD from a single experiment that is representative of at least three replicate experiments. *In vivo* experiments were performed with at least 8 mice/group, which yields a power of >90% to detect any difference among the treatment groups ( $\alpha = 0.05$ ). Significance between experimental *versus* control values was calculated using the Student *t* test.

## RESULTS

**Genetically Modified Lung Cancer Cells Express the *NIS* and *TPO* Genes.** We reported previously that a significant increase in <sup>125</sup>I uptake could be achieved in NSCLC cell lines after transient transfection with the *NIS* gene (12). We also found that cotransfection of the *TPO* gene with *NIS* increased radioiodide uptake and retention in lung cancer cells, and enhanced radiation-induced apoptosis compared

with *NIS* transfection alone (12). To additionally explore the therapeutic potential of *NIS/TPO* gene-based therapy for cancer, we made retroviral constructs that express the *NIS* or *TPO* genes. To allow for selection and characterization of tumor clones, the *NIS* construct contained a hygromycin-resistance gene (pLHCX-*NIS*) and the *TPO* the neomycin-resistance gene (pLNCX-*TPO*). The packaging cell line PT-67 was transfected using a liposomal-based method to generate a high titer of retroviruses expressing functional *NIS* or *TPO* genes. The retroviruses were harvested and used to transduce the human lung poorly differentiated carcinoma cell line H1299. The successful introduction of the *NIS* or both *NIS* and *TPO* genes into the tumor cells was confirmed by RT-PCR with gene-specific primer pairs. Parental lung cancer cells do not express either *NIS* or *TPO* (Fig. 1). In contrast, tumor cells that were transduced with the *NIS* or both *NIS* and *TPO* genes express significant levels of the transduced genes (Fig. 1).

***NIS/TPO*-modified Lung Cancer Cells Markedly Increase <sup>125</sup>I Uptake and Retention.** Forty-two *NIS*-transduced hygromycin-resistant H1299 clones and 63 *NIS/TPO* cotransduced H1299 clones that were both hygromycin- and G418-resistant were isolated. To assess the effectiveness of the *NIS/TPO* gene expression from tumor cells we performed <sup>125</sup>I uptake (Fig. 2A) and retention assays (Fig. 2B). Four of the 42 (9.5%) *NIS*-transduced stable clones had 10–50-fold increase in <sup>125</sup>I uptake, 4 of 42 clones (9.5%) ranged from 5- to 10-fold, 17 of 42 clones (40%) ranged from 1- to 5-fold, whereas the remainder showed no increase. In contrast, 9 of 63 (14.3%) *NIS/TPO* cotransduced stable clones had >100-fold increase in <sup>125</sup>I uptake with the highest <sup>125</sup>I uptake clone up to 320-fold, 9 of 63 (14.3%) clones ranged from 50- to 100-fold, 13 of 63 (20.6%) clones ranged from 10- to 50-fold, 7 of 63 clones (11.1%) ranged from 5- to 10-fold, 11 of 63 clones (15.9%) ranged from 1- to 5-fold, and the remainder had 0 increase. Consistent with previous results (12), inhibition of *NIS* with  $KClO_4$  completely inhibited the increased uptake in both *NIS* and *NIS/TPO* cotransduced clones, indicating that the increased radioiodide uptake was *NIS*-mediated. Three *NIS/TPO* cotransduced clones (*NIS/TPO1*, 2, and 3) in the high <sup>125</sup>I uptake category (an increase in <sup>125</sup>I uptake up to 320X, 170X, and 164X) and the highest <sup>125</sup>I uptake clone transduced by *NIS* (*NIS*, an increase in <sup>125</sup>I uptake up to 17 times) were chosen for <sup>125</sup>I retention assays. After the removal of <sup>125</sup>I, the remaining cell-associated radioactivity of each sample at various time points (5–30 min) was measured. All three of the *NIS/TPO* cotransduced H1299 clones had enhanced radioiodide retention capacity in addition to markedly increased <sup>125</sup>I uptake compared with the *NIS*-transduced clone (31–34% radioiodide retention at 30 min after the removal of <sup>125</sup>I in three *NIS/TPO* clones *versus* only 8% in the *NIS* clone;  $P < 0.01$ ; Fig. 2B). The results additionally confirm our previous findings that *TPO* enhanced *NIS*-mediated radioiodide uptake and retention in NSCLC (12).

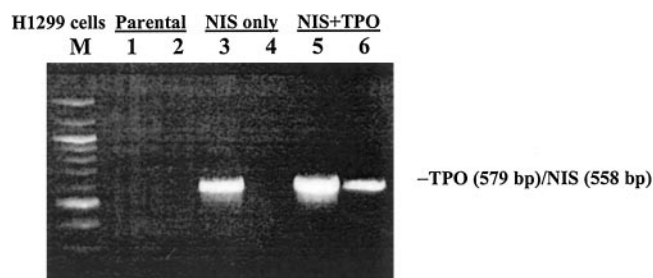


Fig. 1. Expression of *NIS* and *TPO* mRNA in the genetically modified H1299 cells by RT-PCR. *M*, molecular weight marker; *Lanes 1* and *2*, H1299 parental cells; *Lanes 3* and *4*, H1299 cells that were transduced with the *NIS* gene only; *Lanes 5* and *6*, H1299 cells that were transduced with both *NIS* and *TPO* genes; *Lanes 1*, *3*, and *5*, *NIS* expression; *Lanes 2*, *4*, and *6*, *TPO* expression.

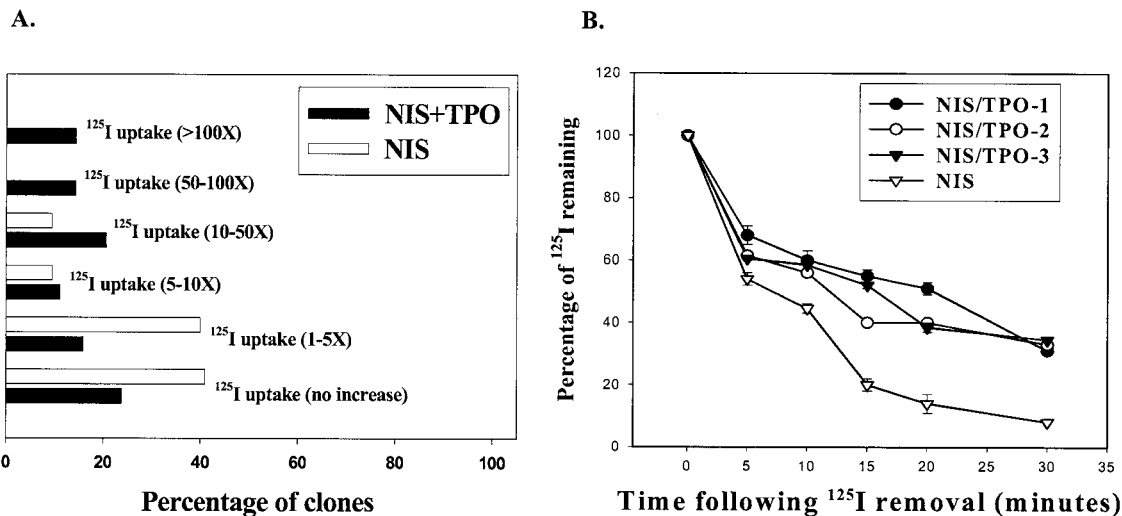


Fig. 2. *NIS/TPO*-modified H1299 cells markedly increased  $^{125}\text{I}$  uptake and retention. *A*, *NIS*- or both *NIS/TPO*-modified cell clones were categorized as >100 $\times$ , 50–100 $\times$ , 10–50 $\times$ , 5–10 $\times$ , 1–5 $\times$ , and no increase based on  $^{125}\text{I}$  uptake levels. *B*, after incubation with  $^{125}\text{I}$  for 1 h, the medium containing radioiodide was removed at various time points (0–30 min). The cell-associated radioactivity was measured with a gamma counter and expressed as percentage of remaining radioactivity versus the original levels (time 0 min). Remaining radioactivity in all three *NIS/TPO* clones was significantly elevated compared with the *NIS* clone ( $P < 0.05$  at time points 5–30 min).

**Nonradioactive Iodide Potently Induces Apoptosis in the *NIS/TPO*-modified Lung Cancer Cells.** Studies showed that iodide excess induces cytotoxicity in thyroid cells (13, 18, 19). To test whether nonradioactive iodide induces apoptosis in genetically modified lung cancer cells, H1299*NIS/TPO* (clone 320X), H1299*NIS* (clone 17X), and parental H1299CV clones were incubated in the presence of 30 mM KI for 48 h, and apoptosis was assessed by the APOPercentage assay method. KI induced apoptosis in >95% of H1299*NIS/TPO* cells (Fig. 3A) but <1% of H1299*NIS* and H1299CV cells (Fig. 3, B and C) underwent apoptosis. In contrast, KCl in the same molar concentration had no significant toxic effect on H1299*NIS/TPO* cells (Fig. 3D), indicating that the cell death in the H1299*NIS/TPO* cells was not because of potassium toxicity.

***NIS/TPO*-modified Tumor Xenografts Markedly Increase  $^{125}\text{I}$  Uptake in SCID Mice.** On the basis of the capacity of *NIS/TPO*-modified lung cancer cells to markedly increase in  $^{125}\text{I}$  uptake *in vitro*, we

tested whether the H1299 xenograft tumors, which were genetically modified with both *NIS* and *TPO* genes (H1299 *NIS/TPO*, clone X320), *NIS* gene alone (H1299 *NIS*, clone 17X), or empty vector as controls (H1299CV) could increase  $^{125}\text{I}$  uptake *in vivo*. Three h after administration of  $^{125}\text{I}$  (1  $\mu\text{Ci}/\text{mouse}$ ) by i.p. injection, tumors from each group of mice were removed, weighed, and the tumor-associated radioactivity was determined by a gamma counter. Consistent with our *in vitro* findings, the highest  $^{125}\text{I}$  uptake was observed in tumors expressing both *NIS* and *TPO* genes ( $P < 0.001$ , compared with control vector-modified tumors; Fig. 4). The *NIS*-modified tumors also had a significant increase in  $^{125}\text{I}$  uptake compared with the control vector-modified tumors ( $P < 0.01$ ; Fig. 4). However, the increase in  $^{125}\text{I}$  uptake in the *NIS*-modified tumors was less than the *NIS/TPO*-modified tumors ( $P < 0.01$ ). The results suggest that the *NIS/TPO*-modified tumor xenografts are capable of concentrating significantly higher levels of iodide *in vivo* compared with the *NIS*-modified tumor xenografts.

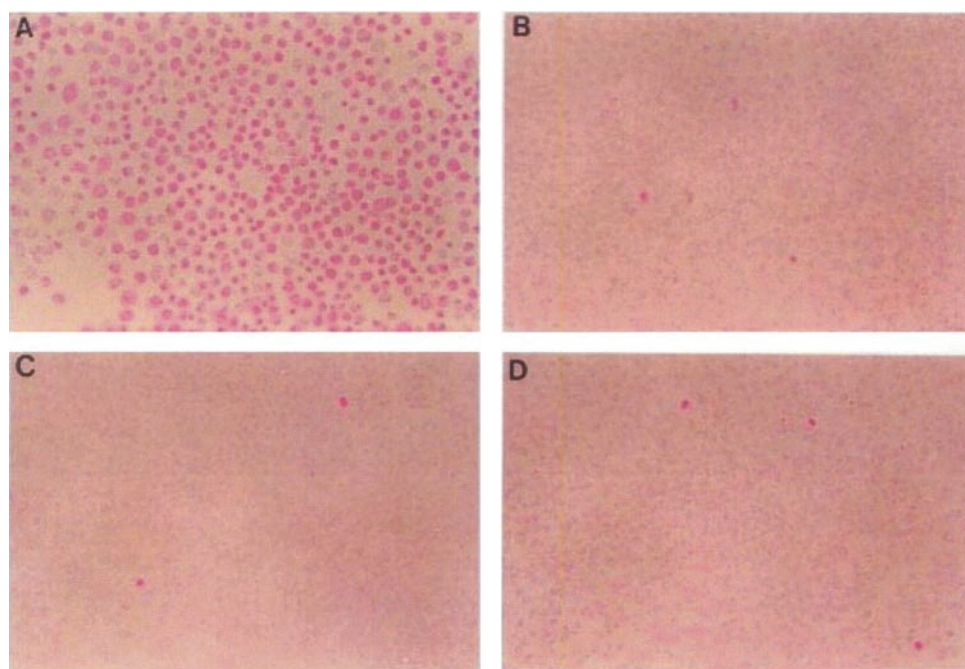


Fig. 3. KI induces apoptosis in >95% H1299*NIS/TPO* cells after a 48-h incubation. *A*, H1299*NIS/TPO* cells in KI; *B*, H1299CV cells in KI; *C*, H1299*NIS* cells in KI; *D*, H1299*NIS/TPO* cells in KCl. Apoptotic cells were stained red, whereas viable cells remain unstained or pale pink.

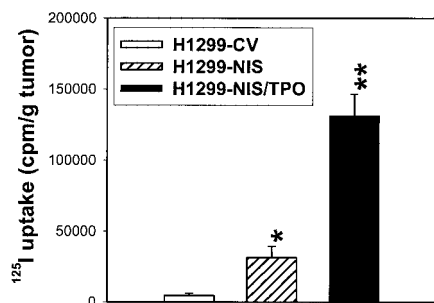


Fig. 4. *NIS/TPO*-modified tumor xenografts show marked increase in <sup>125</sup>I uptake *in vivo*. Three h after administration of <sup>125</sup>I (1 μCi/mouse) by i.p. injection, tumors from each group (n = 8) of mice were removed, weighed, and the tumor-associated radioactivity was determined by a gamma counter. The results were expressed as the mean; bars, ±SD. \*, P < 0.05; \*\*, P < 0.01 compared with the controls.

**Nonradioactive Iodide Effectively Limits the Growth of *NIS/TPO*-modified Tumor Xenografts in SCID Mice.** On the basis of our results indicating that nonradioactive iodide potently induces apoptosis in the *NIS/TPO*-modified lung cancer cells *in vitro*, we evaluated the effect of iodide on genetically modified tumor growth in a murine model. Five × 10<sup>6</sup> of H1299 cells modified with both *NIS* and *TPO* genes (H1299*NIS/TPO*, clones X164 and X320 in duplicate experiments) or empty vectors as controls (H1299CV) were implanted via s.c. injection in the right suprascapular region in SCID mice. When the tumors were ~5 mm in diameter, KI (5 mg/mouse/day) was administered five times per week by i.p. injection. The potential adverse effects of KI were monitored by daily observation of the mice. No significant adverse effects were noted in the mice receiving KI except for minor skin irritation at the injection site. Tumor growth was monitored and documented twice a week. After treatment with KI, a marked reduction of tumor volume was evident only in mice bearing the *NIS/TPO*-modified tumors (Fig. 5A). KI had no effect on tumor volume in mice bearing empty vector-modified tumor xenografts, indicating the critical roles of *NIS* and *TPO* genes. Mice were euthanized at day 26 of KI administration, and tumors from each group were isolated, weighed, and photographed (Fig. 5B). Whereas no statistical differences in tumor weights were noted in the H1299CV (mean = 0.9788 ± 0.1798 g), H1299CV+KI (mean = 0.9504 ± 0.2785 g), and H1299*NIS/TPO* (mean = 1.2829 ± 0.2220 g) groups, KI treatment markedly reduced tumor weight in mice bearing H1299*NIS/TPO* tumors (mean = 0.4031 ± 0.1482g; P < 0.001). The results indicate that non-radioactive iodide effectively limits the growth of *NIS/TPO*-modified tumor xenografts in SCID mice.

**Apoptosis Plays an Important Role in the Iodide-mediated Antitumor Effect *in Vivo*.** To quantify apoptotic events in paraffin-embedded tumor sections, we used a Klenow-FragEL DNA fragmentation detection method to determine apoptotic index. The tumor apoptotic index was expressed as percentage of brown-stained squares divided by total squares examined. Using this method, a higher apoptotic index indicates more extensive apoptosis in tumors examined. The apoptotic index for untreated H1299*NIS/TPO* tumors (clone 320X) was 0.15 and 0.48 after KI treatment (P < 0.001). Morphologically, the untreated H1299*NIS/TPO* tumor sections under low-power (×4 objective) examination revealed large tumor masses with scattered brown-stained areas (Fig. 6A). In contrast, the KI-treated mice bearing H1299*NIS/TPO* tumors showed extensive cell death (Fig. 6B). The corresponding brown areas in H&E sections under high-power (×20 objective) examination showed amorphous necrotic debris in the untreated H1299*NIS/TPO* tumors (Fig. 6C) and clearly demonstrated groups of cells undergoing apoptosis with features of nuclear and cytoplasmic condensation within the necrotic areas in the KI-treated H1299*NIS/TPO* tumors (Fig. 6D). The necrotic areas of the

untreated H1299*NIS/TPO* tumor sections showed faintly stained cell “ghosts” without nuclear details (Fig. 6E). In comparison, the apoptotic cells within the necrotic areas were strongly stained in the KI-treated H1299*NIS/TPO* tumors (Fig. 6F).

**Iodide Induces an Increase in ROS Level and Iodide-induced Apoptosis Is Sensitive to *N*-Acetylcysteine Inhibition.** Iodide-induced apoptosis in the *NIS/TPO*-modified NSCLC cells was associated with DNA damage as early as 12–24 h as determined by TUNEL assays (data not shown). ROS are well known to cause oxidative damage to DNA (20–24). Vitale *et al.* (13) have shown that ROS level was markedly increased during KI treatment in human thyroid cells. To evaluate whether ROS were generated in the *NIS/TPO*-modified NSCLC cells (clone 320X) during KI treatment, cells were incubated in a range of KI concentrations (0–30 mM) for 24 h. Ten μM DCFH-DA was added to the culture and cells were incubated for 1 h before FACS analysis. The results showed that KI induced a marked increase in ROS level in a dose-dependent manner (Fig. 7, A–D). To define whether an increase in ROS level during KI treatment leads to apoptosis, the *NIS/TPO*-modified NSCLC cells were incubated in a range of KI concentrations (0–30 mM) in the absence or presence of *N*-acetylcysteine (5 μM). Preliminary studies showed that *N*-acetylcysteine (5 μM) is not toxic to NSCLC cells and provides optimal antioxidant effect (data not shown). After a 48-h incubation,

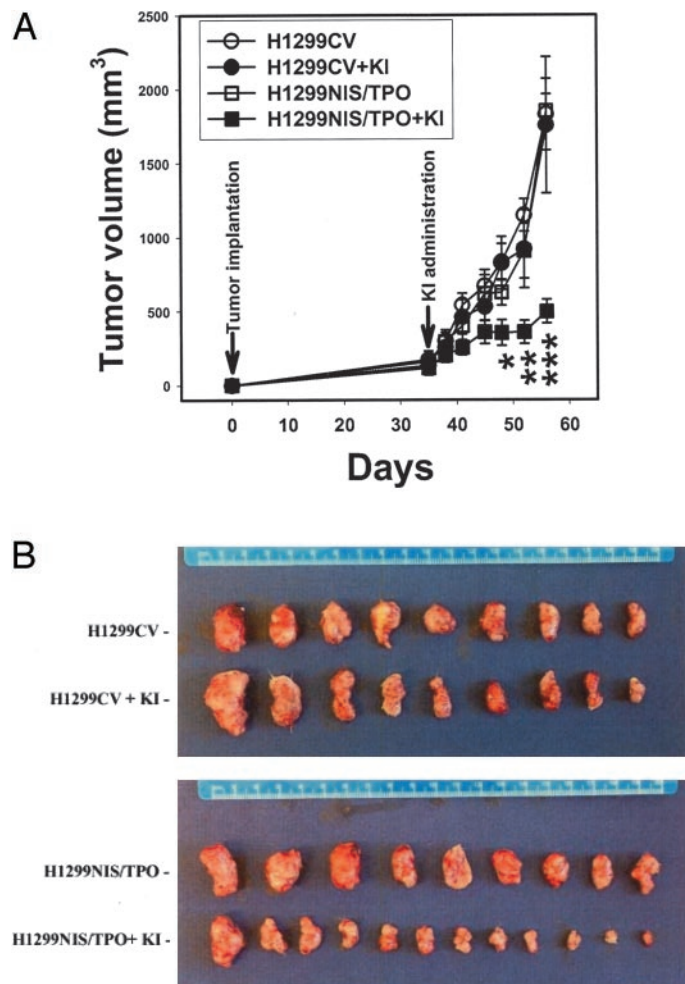


Fig. 5. Nonradioactive iodide effectively limits the growth of *NIS/TPO*-modified tumor xenografts in SCID mice. A, KI markedly reduces tumor volume in *NIS/TPO*-modified tumor xenografts. \*, P < 0.05; \*\*, P < 0.01; \*\*\*, P < 0.001 compared with nontreated H1299*NIS/TPO* tumors. B, photographs of tumors from each group of mice. H1299CV, n = 9; H1299CV+KI, n = 9; H1299*NIS/TPO*, n = 9; H1299*NIS/TPO*+KI, n = 12; bars, ±SD.

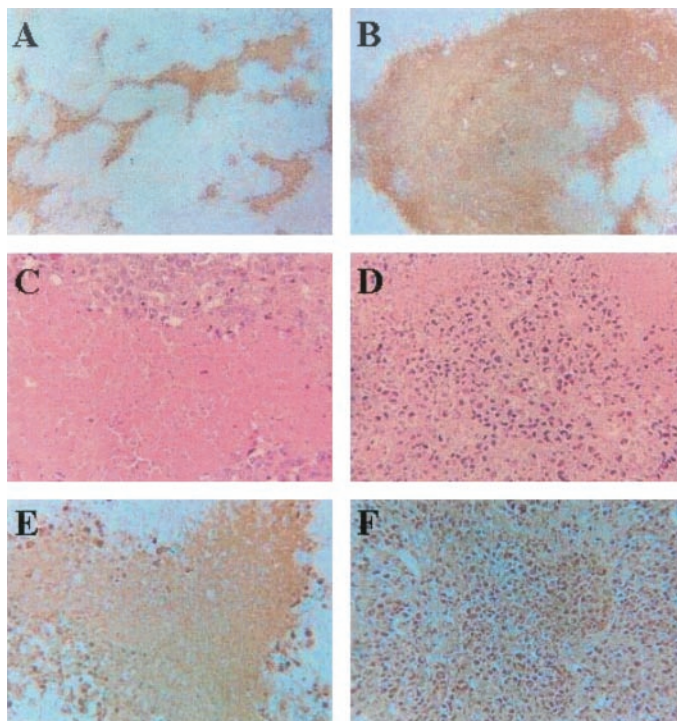


Fig. 6. Apoptosis plays an important role in the iodide-mediated antitumor effect *in vivo*. The apoptotic/necrotic cells stain brown, whereas healthy living cells remain unstained with the Klenow-FragEL method. A, untreated H1299NIS/TPO tumors showed scattered brown-stained areas (Klenow-FragEL, original magnification  $\times 40$ ); B, H1299NIS/TPO tumors with KI treatment showed extensive cell death (Klenow-FragEL, original magnification  $\times 40$ ); C, untreated H1299NIS/TPO tumors showed amorphous necrotic debris (H&E, original magnification  $\times 200$ ); D, H1299NIS/TPO tumors with KI treatment clearly demonstrated groups of cells undergoing apoptosis with features of nuclear and cytoplasmic condensation within the necrotic areas (H&E, original magnification  $\times 200$ ); E, necrotic debris was stained faintly in untreated H1299NIS/TPO tumors (Klenow-FragEL, original magnification  $\times 200$ ); F, apoptotic cells were strongly stained in H1299NIS/TPO tumor sections with KI treatment (Klenow-FragEL, original magnification  $\times 200$ ).

apoptosis was quantified by measuring the amount of released NMP in the culture supernatants from apoptotic cells by NMP assays. The results showed that *N*-acetylcysteine potently inhibits iodide-induced apoptosis (Fig. 7E, \*,  $P < 0.01$ ).

**Iodide-induced Apoptosis Is Associated with Overexpression of CDKN1A and Down-Regulation of Survivin.** To begin to identify potential pathways involved in iodide-induced apoptosis in the *NIS/TPO*-modified lung cancer cells, we performed gene array analysis in the *NIS/TPO*-modified NSCLC cells after a 24-h KI treatment. Among the genes studied, overexpression of *CDKN1A* and down-regulation of *survivin* were associated with iodide-induced apoptosis in the *NIS/TPO*-modified NSCLC cells. The expression levels of other apoptosis-associated genes such as *p53*, *Bcl-2*, caspases, and ataxia telangiectasia mutated (*ATM*) pathway genes were not modified. In addition, death ligands and receptors, such as TNF ligand, TNF receptor, TNF-associated factor, death domain, and death effector domain families were not altered. Other genes associated with apoptosis signaling, DNA damage and repair, other members of the growth arrest/senescence family, or other members of the inhibitors of apoptosis family did not show significant changes in expression levels (data not shown). Consistent with the expression levels of *CDKN1A* and *survivin* mRNAs, an increase in *CDKN1A* and a decrease in *survivin* proteins in response to iodide-induced apoptosis were demonstrated in the *NIS/TPO*-modified lung cancer cells (clones 320X, 164X, and 170X) by specific ELISA (Fig. 8, A and B; \*,  $P < 0.05$ ; \*\*,  $P < 0.01$ ). Kinetic studies of *CDKN1A* in the *NIS/TPO*-modified lung

cancer cells (clones 164X and 320X) showed that *CDKN1A* increased to a maximal level as early as 8 h after KI supplement and maintained this high level up to 48 h. In comparison, *survivin* level started to decrease as early as 12 h after KI supplement, and a maximal reduction of *survivin* was evident at 24–48 h (data not shown).

**DISCUSSION**

*NIS* expression mediates the therapeutic efficacy of radioiodide in thyroid diseases (25, 26). Endogenous *NIS* expression has not been found in normal lung tissue or lung cancer (27). Transfection of the *NIS* gene into a variety of malignancies, including melanoma, colon carcinoma, ovarian adenocarcinoma, and lung and prostate cancers, confers radioiodide uptake (28–30). Introduction of the *TPO* gene alone into human anaplastic thyroid carcinoma cells provided no significant increase in  $^{125}\text{I}$  uptake, although the *TPO* expression in the genetically modified cell line was 1800-fold above the background levels (31).

$^{131}\text{I}$  therapy is the standard treatment for well-differentiated thyroid cancers that express the *NIS* gene (26). Endogenous *NIS* expression or induced expression after retinoic acid stimulation may mediate effective radioiodide therapy in breast cancer (9, 32, 33). Because the treatment is very effective for thyroid cancer, Mandell *et al.* (28)

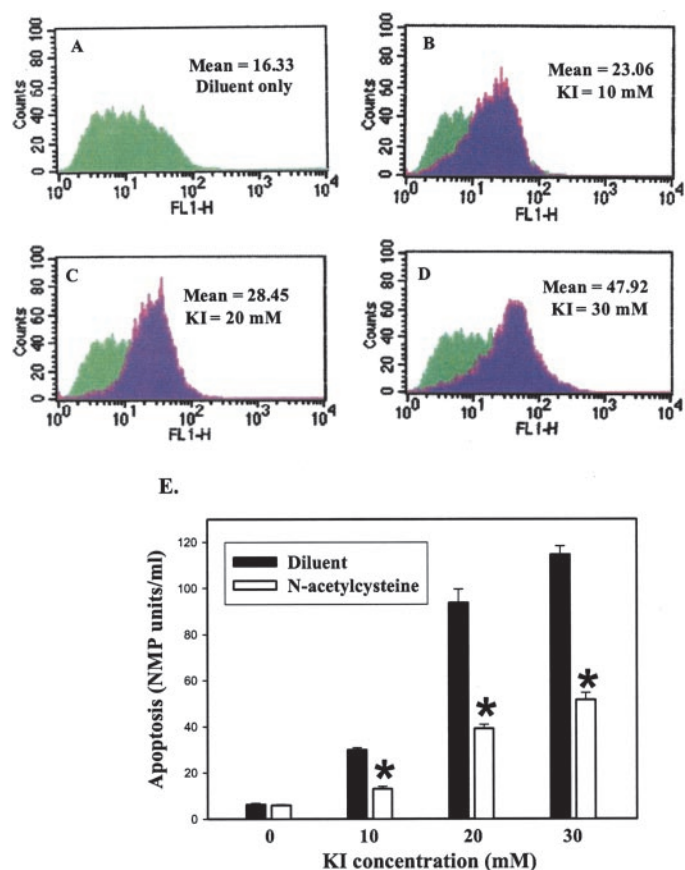
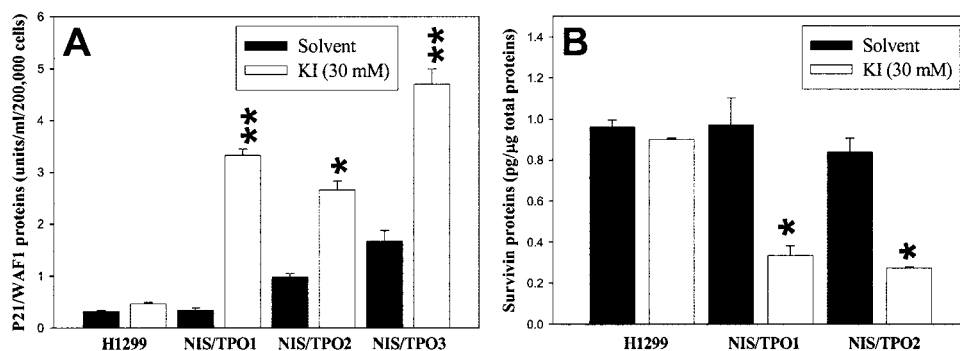


Fig. 7. Iodide induces an increase in ROS level and iodide-induced apoptosis is sensitive to *N*-acetylcysteine inhibition. The *NIS/TPO*-modified NSCLC cells were treated with variable concentration of KI (A, diluent only; B, 10 mM; C, 20 mM; D, 30 mM) for 24 h. Cells were then incubated with DCFH-DA for 1 h and analyzed by FACScan. The green peaks (A–D) show the background level of mean fluorescence in cells receiving diluent only. The purple peaks (A–D) demonstrate a progressive shift of mean fluorescence intensity to the high end in cells when KI supplement is increased. The purple peak overlaps the green peak when KI concentration is reduced to 5 mM (data not shown). E, the *NIS/TPO* modified NSCLC cells were treated with variable concentration of KI (0–30 mM) in the absence or presence of *N*-acetylcysteine (5 mM) for 48 h. The culture medium from each sample was collected for NMP ELISA. \*,  $P < 0.01$ ; bars,  $\pm$ SD.

Fig. 8. Iodide-induced apoptosis is associated with overexpression of *CDKN1A* and down-regulation of survivin. **A**, an increase in *CDKN1A* proteins after incubation with 30 mM KI for 24 h was observed in three *NIS/TPO* clones tested by ELISA. **B**,  $\pm$  a decrease in survivin proteins after incubation with 30 mM KI for 24 h was demonstrated by ELISA in two *NIS/TPO* clones tested. Control cultures received solvent only. The results are expressed as the mean; bars,  $\pm$ SD. \*,  $P < 0.05$ ; \*\*,  $P < 0.01$  compared with the controls.



initially proposed *NIS*-based radioisotope concentrator gene therapy for extrathyroidal malignancies. We reported previously that the peak  $^{125}\text{I}$  uptake occurred rapidly, and cells maintained a high steady-state intracellular concentration provided that radioiodide was present in the medium (12). However, if radioiodide was removed from the medium, the cells displayed a rapid loss of iodide, suggesting that there was a pronounced egress of radioiodide. This led us to conclude that the cytotoxic efficacy of *NIS* gene transfer may be limited by radioiodide efflux in lung cancer cells and that enhancing the intracellular retention of radioiodide may confer a therapeutic advantage.

We developed a strategy to introduce the *NIS* gene into tumor cells to promote radioiodide uptake and the *TPO* gene to enhance retention of radioiodide by promoting its organification (12). Our rationale for choosing the *NIS* and *TPO* genes is that intracellular concentration of iodide in the normal thyroid is determined by a balance between *NIS*-mediated iodide influx and *TPO*-promoted iodide organification (25, 26, 34–36). An increase in radioiodinated intracellular proteins that was sensitive to methimazole inhibition in the *NIS/TPO* cotransfected NSCLC cells correlated with an improved radioiodide uptake and retention, suggesting that an increase in intracellular  $^{125}\text{I}$  concentration was attributable to *TPO*-mediated organification (12). Because the substrates for *TPO* in NSCLC may not be the same as those in the thyroid cells, *TPO* presumably uses other tyrosine-rich protein substrates to achieve efficient iodination of intracellular proteins in the *NIS/TPO*-transfected lung cancer cells. Furthermore, the therapeutic efficacy of radioiodide incorporation may not be affected in other cancers such as breast cancer, because the efflux of radioiodide is relatively slow (32). Results in the current study from single clones that stably express *NIS* or both *NIS* and *TPO* genes by retroviral transduction additionally confirm our previous findings (12).

We demonstrated previously radiation-induced apoptosis in lung cancer cells using the *NIS/TPO* system *in vitro* (12). Although this novel strategy may have therapeutic potential for locally advanced solid tumor, radiation-induced toxicity to normal tissues could limit its clinical application. Consistent with previous studies in thyroid cells (13, 18, 19), our results indicate that nonradioactive iodide potently induces apoptosis in the *NIS/TPO*-modified lung cancer cells *in vitro* and *in vivo*. Hao *et al.* (37) have shown that administration of nonradioactive iodide after radioactive iodide therapy in patients with Graves' disease is safe and effective. On the basis of these findings, we determined whether the growth of the *NIS/TPO*-modified human tumors could be controlled by the administration of nonradioactive iodide *in vivo*. Results in the current study show that *NIS/TPO*-modified lung cancer cells *in vitro* and tumor xenografts *in vivo* significantly concentrate therapeutic levels of nonradioactive iodide resulting in enhanced apoptosis.

We repeated apoptosis studies using different methods including flow cytometry (data not shown), TUNEL assays (Fig. 6) and NMP assays (Fig. 7), and confirmed the above results. Furthermore, we

performed apoptosis studies in different *NIS/TPO*-modified NSCLC cell lines and different clones from the same cell line with variable levels of  $^{125}\text{I}$  uptake. Nonradioactive iodide-induced apoptosis was directly related to the level of  $^{125}\text{I}$  uptake without significant cell line preference in NSCLC (data not shown). Whereas clones in the low or moderate  $^{125}\text{I}$  uptake categories (an increase in  $^{125}\text{I}$  uptake <10 times or 10–50 times) did not show significant apoptosis, all of the clones in the high  $^{125}\text{I}$  uptake category (an increase in  $^{125}\text{I}$  uptake >100 times) underwent marked apoptosis after a 48-h incubation in KI (Fig. 3).<sup>4</sup> Clones in the moderately high category (an increase in  $^{125}\text{I}$  uptake 50–100 times) showed statistically significant apoptosis *in vitro* compared with the controls (data not shown). The efficacy of nonradioactive iodide-induced tumor volume reduction *in vivo* in the moderately high category has not been determined and requires additional investigation. In addition, kinetic studies of nonradioactive iodide-induced apoptosis in the *NIS/TPO*-modified lung cancer cells (clones 164X and 320X) showed a slight but statistically significant increase in apoptosis that was evident as early as 12 h after KI supplement and reached a maximal level at 48–72 h (95–100% cell death; data not shown).

Iodide administration is associated with a variety of potential complications. The most prominent side effect of iodide is salivary gland inflammation (38, 39). We obtained salivary gland specimens from mice with or without KI treatment. No acute or chronic inflammation was noted in the histological sections from the KI-treated group compared with the controls (data not shown). Another reported effect of iodide is stimulation of autonomous thyroid hormone production (Jod-basetow syndrome; Ref. 40). Most susceptible patients could be identified by screening for underlying nodular thyroid disease. Finally, a “down-regulation” of iodide-uptake is seen in the thyroid after iodide exposure (Wolff-Chaikoff effect). This was shown recently to be related to down-regulation of *NIS* expression (41). *NIS* and *TPO* expression in genetically modified tumors is autonomous and under the control of their own promoters, independent of plasma iodide levels.

Thyroid toxicity of iodide excess has been demonstrated previously *in vitro* and *in vivo* (13, 19, 42). The potential mechanisms of iodide-induced apoptosis in thyroid cells were proposed in connection to the overproduction of ROS by oxidation of excess intracellular iodide (13). Oxidative stress occurs in cells when the generation of ROS overwhelms the natural antioxidant defenses of the cell. There is a growing consensus that oxidative stress and the antioxidant state of a cell plays a pivotal role in regulating apoptosis (20–24). Consistent with previous observation by others in thyroid cells (13), iodide markedly induced ROS in a dose-dependent manner in the *NIS/TPO* modified NSCLC cells (Fig. 7, A–D). Antioxidants such as *N*-acetyl-

<sup>4</sup> Unpublished observations.

cysteine have been used as tools for investigating the role of ROS in numerous biological and pathological processes (43). The current study using *N*-acetylcysteine as an antioxidant to counteract the effect of ROS suggests that ROS may play an important role in iodide-induced apoptosis (Fig. 7E).

*CDKN1A* is one of the key proteins involved in growth arrest/senescence through the inhibition of cell cycle progression at the G<sub>2</sub>/M phase (44–49). A member of inhibitors of apoptosis family, survivin is expressed in many malignancies including NSCLC (50–54). Survivin has been shown to interfere with *CDKN1A* function, and suppresses cell death signaling (55, 56). In a recently reported clinical trial, up-regulation of *CDKN1A* and down-regulation of survivin were observed in tumor biopsy specimens in response to combination therapy with wild-type *p53* gene transfer and gemcitabine (57). This dual modulation of both *CDKN1A* and survivin gene expression was also demonstrated in the current study. A functional connection between *CDKN1A* and ROS has been suggested previously (58–62). The importance of *CDKN1A*, and *survivin*, and the relationship between ROS and these two signal mediators involved in iodide-induced apoptosis, currently remain unclear and require additional investigation.

The results of this study indicate that a therapeutic dose of nonradioactive iodide has potent efficacy and high selectivity against lung cancer cells when used in combination with genetic modification of cancer cells expressing the *NIS/TPO* genes. Nonradioactive iodide could be used as adjuvant therapy to potentially enhance the efficacy and reduce radiation-associated toxicity of <sup>131</sup>I therapy. Clinically, the iodide could be delivered as oral supplements. Our findings suggest a novel therapeutic strategy for the treatment of a broad array of solid tumors with minimal adverse effects. Clinical applications of gene therapy for cancer require advances in gene delivery systems. The ultimate success of gene therapies will depend on gene transfer vectors that facilitate the expression of a specific gene at therapeutic levels in cancer cells without eliciting cytotoxicity. Although we have shown the feasibility of the *NIS/TPO* mechanism using nonradioactive iodide for the reduction of genetically modified tumors, the full potential of this approach awaits the development of new vectors for efficient tumor-specific delivery. In the current study we have used an approach to demonstrate a proof of principle regarding the combination of *NIS/TPO* and nonradioactive iodide. Clinically relevant methods of gene transfer are under investigation, and we are currently evaluating a variety of new gene delivery systems to introduce the *NIS/TPO* genes into tumors *in vivo*. Future studies will test new vector systems for *in vivo* gene delivery and the efficacy of this approach for its therapeutic potential for lung cancer.

## REFERENCES

- Shields, P. G. Molecular epidemiology of smoking and lung cancer. *Oncogene*, *21*: 6870–6876, 2002.
- Thun, M. J., Henley, S. J., and Calle, E. E. Tobacco use and cancer: an epidemiologic perspective for geneticists. *Oncogene*, *21*: 7307–7325, 2002.
- Franceschi, S., and Bidoli, E. The epidemiology of lung cancer. *Ann. Oncol.*, *10* (Suppl. 5): S3–S6, 1999.
- Dai, G., Levy, O., and Carrasco, N. Cloning and characterization of the thyroid iodide transporter. *Nature (Lond.)*, *379*: 458–460, 1996.
- Trapasso, F., Iuliano, R., Chiefari, E., Arturi, F., Stella, A., Filetti, S., Fusco, A., and Russo, D. Iodide symporter gene expression in normal and transformed rat thyroid cells. *Eur. J. Endocrinol.*, *140*: 447–451, 1999.
- Nilsson, M. Molecular and cellular mechanisms of transepithelial iodide transport in the thyroid. *Biofactors*, *10*: 277–285, 1999.
- Spitzweg, C., and Morris, J. C. The sodium iodide symporter: its pathophysiological and therapeutic implications. *Clin. Endocrinol. (Oxf)*, *57*: 559–574, 2002.
- Filetti, S., Bidart, J. M., Arturi, F., Caillou, B., Russo, D., and Schlumberger, M. Sodium/iodide symporter: a key transport system in thyroid cancer cell metabolism. *Eur. J. Endocrinol.*, *141*: 443–457, 1999.
- Tazebay, U. H., Wapnir, I. L., Levy, O., Dohan, O., Zuckier, L. S., Zhao, Q. H., Deng, H. F., Amenta, P. S., Fineberg, S., Pestell, R. G., and Carrasco, N. The mammary gland iodide transporter is expressed during lactation and in breast cancer. *Nat. Med.*, *6*: 871–878, 2000.
- Ohtaki, S., Nakagawa, H., Nakamura, M., and Kotani, T. Thyroid peroxidase: experimental and clinical integration. *Endocr. J.*, *43*: 1–14, 1996.
- McLachlan, S. M., and Rapoport, B. The molecular biology of thyroid peroxidase: cloning, expression and role as autoantigen in autoimmune thyroid disease. *Endocr. Rev.*, *13*: 192–206, 1992.
- Huang, M., Batra, R. K., Kogai, T., Lin, Y. Q., Hershman, J. M., Lichtenstein, A., Sharma, S., Zhu, L. X., Brent, G. A., and Dubinett, S. M. Ectopic expression of the thyroperoxidase gene augments radioiodide uptake and retention mediated by the sodium iodide symporter in non-small cell lung cancer. *Cancer Gene Ther.*, *8*: 612–618, 2001.
- Vitale, M., Di Matola, T., D'Ascoli, F., Salzano, S., Bogazzi, F., Fenzi, G., Martino, E., and Rossi, G. Iodide excess induces apoptosis in thyroid cells through a p53-independent mechanism involving oxidative stress. *Endocrinology*, *141*: 598–605, 2000.
- Fadok, V. A., Savill, J. S., Haslett, C., Bratton, D. L., Doherty, D. E., Campbell, P. A., and Henson, P. M. Different populations of macrophages use either the vitronectin receptor or the phosphatidylserine receptor to recognize and remove apoptotic cells. *J. Immunol.*, *149*: 4029–4035, 1992.
- Gavrieli, Y., Sherman, Y., and Ben-Sasson, S. A. Identification of programmed cell death *in situ* via specific labeling of nuclear DNA fragmentation. *J. Cell Biol.*, *119*: 493–501, 1992.
- van Dierendonck, J. H. DNA damage detection using DNA polymerase I or its Klenow fragment. Applicability, specificity, limitations. *Methods Mol. Biol.*, *203*: 81–108, 2002.
- Sharma, S., Stolina, M., Zhu, L., Lin, Y., Batra, R., Huang, M., Strieter, R., and Dubinett, S. M. Secondary lymphoid organ chemokine reduces pulmonary tumor burden in spontaneous murine bronchoalveolar cell carcinoma. *Cancer Res.*, *61*: 6406–6412, 2001.
- Golstein, J., and Dumont, J. E. Cytotoxic effects of iodide on thyroid cells: difference between rat thyroid FRTL-5 cell and primary dog thyrocyte responsiveness. *J. Endocrinol. Investig.*, *19*: 119–126, 1996.
- Mahmoud, I., Colin, I., Many, M. C., and Denef, J. F. Direct toxic effect of iodide in excess on iodine-deficient thyroid glands: epithelial necrosis and inflammation associated with lipofuscin accumulation. *Exp. Mol. Pathol.*, *44*: 259–271, 1986.
- Hasnain, S. E., Begum, R., Ramaiah, K. V., Sahdev, S., Shajil, E. M., Taneja, T. K., Mohan, M., Athar, M., Sah, N. K., and Krishnaveni, M. Host-pathogen interactions during apoptosis. *J. Biosci.*, *28*: 349–358, 2003.
- Curtin, J. F., Donovan, M., and Cotter, T. G. Regulation and measurement of oxidative stress in apoptosis. *J. Immunol. Methods.*, *265*: 49–72, 2002.
- Feinendegen, L. E. Reactive oxygen species in cell responses to toxic agents. *Hum. Exp. Toxicol.*, *21*: 85–90, 2002.
- Castedo, M., Ferri, K., Roumier, T., Metivier, D., Zamzami, N., and Kroemer, G. Quantitation of mitochondrial alterations associated with apoptosis. *J. Immunol. Methods.*, *265*: 39–47, 2002.
- Sorescu, D., and Griending, K. K. Reactive oxygen species, mitochondria, and NAD(P)H oxidases in the development and progression of heart failure. *Congest. Heart Fail.*, *8*: 132–140, 2002.
- Braga, M., Walpert, N., Burch, H. B., Solomon, B. L., and Cooper, D. S. The effect of methimazole on cure rates after radioiodine treatment for Graves' hyperthyroidism: a randomized clinical trial. *Thyroid*, *12*: 135–139, 2002.
- Reiners, C., and Farahati, J. I<sup>131</sup>I therapy of thyroid cancer patients. *Q. J. Nucl. Med.*, *43*: 324–335, 1999.
- Ajjan, R. A., Kamaruddin, N. A., Crisp, M., Watson, P. F., Ludgate, M., and Weetman, A. P. Regulation and tissue distribution of the human sodium iodide symporter gene. *Clin. Endocrinol. (Oxf)*, *49*: 517–523, 1998.
- Mandell, R. B., Mandell, L. Z., and Link, C. J., Jr. Radioisotope concentrator gene therapy using the sodium/iodide symporter gene. *Cancer Res.*, *59*: 661–668, 1999.
- Boland, A., Ricard, M., Opolon, P., Bidart, J. M., Yeh, P., Filetti, S., Schlumberger, M., and Perricaudet, M. Adenovirus-mediated transfer of the thyroid sodium/iodide symporter gene into tumors for a targeted radiotherapy. *Cancer Res.*, *60*: 3484–3492, 2000.
- Spitzweg, C., Zhang, S., Bergert, E. R., Castro, M. R., McIver, B., Heufelder, A. E., Tindall, D. J., Young, C. Y., and Morris, J. C. Prostate-specific antigen (PSA) promoter-driven androgen-inducible expression of sodium iodide symporter in prostate cancer cell lines. *Cancer Res.*, *59*: 2136–2141, 1999.
- Haberkmorn, U., Altmann, A., Jiang, S., Morr, I., Mahmut, M., and Eisenhut, M. Iodide uptake in human anaplastic thyroid carcinoma cells after transfer of the human thyroid peroxidase gene. *Eur. J. Nucl. Med.*, *28*: 633–638, 2001.
- Kogai, T., Schultz, J. J., Johnson, L. S., Huang, M., and Brent, G. A. Retinoic acid induces sodium/iodide symporter gene expression and radioiodide uptake in the MCF-7 breast cancer cell line. *Proc. Natl. Acad. Sci. USA*, *97*: 8519–8524, 2000.
- Zuckier, L. S., Dadachova, E., Dohan, O., and Carrasco, N. The endogenous mammary gland Na<sup>(+)</sup>/I<sup>(-)</sup> symporter may mediate effective radioiodide therapy in breast cancer. *J. Nucl. Med.*, *42*: 987–988, 2001.
- Taugog, A., Dorris, M. L., and Doerge, D. R. Mechanism of simultaneous iodination and coupling catalyzed by thyroid peroxidase. *Arch. Biochem. Biophys.*, *330*: 24–32, 1996.
- Morrison, M., and Schonbaum, G. R. Peroxidase-catalyzed halogenation. *Annu. Rev. Biochem.*, *45*: 861–888, 1976.
- Edwards, H. H., and Morrison, M. Localization of thyroid peroxidase and the site of iodination in rat thyroid gland. *Biochem. J.*, *158*: 477–479, 1976.
- Hao, S. T., Reasner, C. A., II, and Becker, R. A. Use of cold iodine in patients with Graves' disease: observations from a clinical practice. *Endocr. Pract.*, *7*: 438–442, 2001.

38. Kalaria, V. G., Porsche, R., and Ong, L. S. Iodide mumps: acute sialadenitis after contrast administration for angioplasty. *Circulation*, *104*: 2384, 2001.
39. Acquaviva, G., Galluzzo, M., Millarelli, S., Miele, V., and De Lillo, M. L. Salivary glands swelling after the administration of a non-ionic iodized contrast medium. *Acta Otorhinolaryngol. Ital.*, *20*: 125–128, 2000.
40. El-Shirbiny, A. M., Stavrou, S. S., Dnistrian, A., Sonenberg, M., Larson, S. M., and Divgi, C. R. Jod-Basedow syndrome following oral iodine and radioiodinated-antibody administration. *J. Nucl. Med.*, *38*: 1816–1817, 1997.
41. Eng, P. H., Cardona, G. R., Fang, S. L., Previti, M., Alex, S., Carrasco, N., Chin, W. W., and Braverman, L. E. Escape from the acute Wolff-Chaikoff effect is associated with a decrease in thyroid sodium/iodide symporter messenger ribonucleic acid and protein. *Endocrinology*, *140*: 3404–3410, 1999.
42. Belshaw, B. E., and Becker, D. V. Necrosis of follicular cells and discharge of thyroidal iodine induced by administering iodide to iodine-deficient dogs. *J. Clin. Endocrinol. Metab.*, *36*: 466–474, 1973.
43. Zafarullah, M., Li, W. Q., Sylvester, J., and Ahmad, M. Molecular mechanisms of N-acetylcysteine actions. *Cell Mol. Life Sci.*, *60*: 6–20, 2003.
44. Chang, B. D., Swift, M. E., Shen, M., Fang, J., Broude, E. V., and Roninson, I. B. Molecular determinants of terminal growth arrest induced in tumor cells by a chemotherapeutic agent. *Proc. Natl. Acad. Sci. USA*, *99*: 389–394, 2002.
45. el-Deiry, W. S., Tokino, T., Velculescu, V. E., Levy, D. B., Parsons, R., Trent, J. M., Lin, D., Mercer, W. E., Kinzler, K. W., and Vogelstein, B. WAF1, a potential mediator of p53 tumor suppression. *Cell*, *75*: 817–825, 1993.
46. Harper, J. W., Adami, G. R., Wei, N., Keyomarsi, K., and Elledge, S. J. The p21 Cdk-interacting protein Cip1 is a potent inhibitor of G1 cyclin-dependent kinases. *Cell*, *75*: 805–816, 1993.
47. Xiong, Y., Hannon, G. J., Zhang, H., Casso, D., Kobayashi, R., and Beach, D. p21 is a universal inhibitor of cyclin kinases. *Nature (Lond.)*, *366*: 701–704, 1993.
48. Gu, Y., Turck, C. W., and Morgan, D. O. Inhibition of CDK2 activity *in vivo* by an associated 20K regulatory subunit. *Nature (Lond.)*, *366*: 707–710, 1993.
49. Li, R., Waga, S., Hannon, G. J., Beach, D., and Stillman, B. Differential effects by the p21 CDK inhibitor on PCNA-dependent DNA replication and repair. *Nature (Lond.)*, *371*: 534–537, 1994.
50. Hofmann, H. S., Simm, A., Hammer, A., Silber, R. E., and Bartling, B. Expression of inhibitors of apoptosis (IAP) proteins in non-small cell human lung cancer. *J. Cancer Res. Clin. Oncol.*, *128*: 554–560, 2002.
51. Nicholson, D. W., and Thornberry, N. A. Apoptosis. Life and death decisions. *Science (Wash. DC)*, *299*: 214–215, 2003.
52. Wall, N. R., O'Connor, D. S., Plescia, J., Pommier, Y., and Altieri, D. C. Suppression of survivin phosphorylation on Thr34 by flavopiridol enhances tumor cell apoptosis. *Cancer Res.*, *63*: 230–235, 2003.
53. Joseph, B., Lewensohn, R., and Zhivotovsky, B. Role of apoptosis in the response of lung carcinomas to anti-cancer treatment. *Ann. N. Y. Acad. Sci.*, *926*: 204–216, 2000.
54. Xia, C., Xu, Z., Yuan, X., Uematsu, K., You, L., Li, K., Li, L., McCormick, F., and Jablons, D. M. Induction of apoptosis in mesothelioma cells by antisurvivin oligonucleotides. *Mol. Cancer Ther.*, *1*: 687–694, 2002.
55. Suzuki, A., Ito, T., Kawano, H., Hayashida, M., Hayasaki, Y., Tsutomi, Y., Akahane, K., Nakano, T., Miura, M., and Shiraki, K. Survivin initiates procaspase 3/p21 complex formation as a result of interaction with Cdk4 to resist Fas-mediated cell death. *Oncogene*, *19*: 1346–1353, 2000.
56. Li, F., Ackermann, E. J., Bennett, C. F., Rothermel, A. L., Plescia, J., Tognin, S., Villa, A., Marchisio, P. C., and Altieri, D. C. Pleiotropic cell-division defects and apoptosis induced by interference with survivin function. *Nat. Cell Biol.*, *1*: 461–466, 1999.
57. Wen, S. F., Mahavni, V., Quijano, E., Shinoda, J., Grace, M., Musco-Hobkinson, M. L., Yang, T. Y., Chen, Y., Runnenbaum, I., Horowitz, J., Maneval, D., Hutchins, B., and Buller, R. Assessment of p53 gene transfer and biological activities in a clinical study of adenovirus-p53 gene therapy for recurrent ovarian cancer. *Cancer Gene Ther.*, *10*: 224–238, 2003.
58. Helt, C. E., Rancourt, R. C., Stavarsky, R. J., and O'Reilly, M. A. p53-dependent induction of p21(Cip1/WAF1/Sdi1) protects against oxygen-induced toxicity. *Toxicol. Sci.*, *63*: 214–222, 2001.
59. Roy, S., Khanna, S., Bickerstaff, A. A., Subramanian, S. V., Atalay, M., Bierl, M., Pendyala, S., Levy, D., Sharma, N., Venojarvi, M., Strauch, A., Orosz, C. G., and Sen, C. K. Oxygen sensing by primary cardiac fibroblasts: a key role of p21(Waf1/Cip1/Sdi1). *Circ. Res.*, *92*: 264–271, 2003.
60. Macip, S., Igarashi, M., Fang, L., Chen, A., Pan, Z. Q., Lee, S. W., and Aaronson, S. A. Inhibition of p21-mediated ROS accumulation can rescue p21-induced senescence. *EMBO J.*, *21*: 2180–2188, 2002.
61. Yin, Y., Solomon, G., Deng, C., and Barrett, J. C. Differential regulation of p21 by p53 and Rb in cellular response to oxidative stress. *Mol. Carcinog.*, *24*: 15–24, 1999.
62. Jin, G. F., Hurst, J. S., and Godley, B. F. Rod outer segments mediate mitochondrial DNA damage and apoptosis in human retinal pigment epithelium. *Curr. Eye Res.*, *23*: 11–19, 2001.